

Search-Efficient Methods of Detection of Cyclostationary Signals

Grace K. Yeung and William A. Gardner, *Fellow, IEEE*

Abstract—Conventional signal processing methods that exploit cyclostationarity for the detection of weak signals in noise require fine resolution in cycle frequency for long integration time. Hence, in cases of weak-signal detection and broadband search, problems in implementation, such as excessive computational complexity and storage and search arise. This paper introduces two new search-efficient methods of cycle detection, namely the autocorrelated cyclic autocorrelation (ACA) and the autocorrelated cyclic periodogram (ACP) methods. For a given level of performance reliability, the ACA and ACP methods allow much larger resolution width in cycle frequency to be used in their implementations, compared to the conventional methods of cyclic spectral analysis. Thus, the amount of storage and search can be substantially reduced. Analyses of the two methods, performance comparison, and computer simulation results are presented.

I. INTRODUCTION

THE PROBLEM of searching for weak radio communications and telemetry signals buried in noise arises in many areas of engineering and science. The common approach to the detection of these signals is based on radiometry, which is measurement of received energy in selected time and frequency intervals. However, the presence of variable background noise and interference that overlap in time and frequency with the signal of interest (SOI) makes the task of detecting weak signals using these conventional energy-detection methods difficult and, in some cases, impossible [1]. Therefore, new detection schemes as well as methods for improving the performance of existing schemes are continually being sought.

Meanwhile, continuing research efforts in the area of cyclostationarity and growing applications of this signal property, which is inherent in many man-made signals such as communications signals, have made evident the fact that methods exploiting cyclostationarity have many advantages over conventional radiometric methods for purposes of signal interception [1]. The detection of cyclostationary signals involves cyclic spectral analysis (or, equivalently, spectral correlation analysis) of the received data. Conventional methods of cyclic spectral analysis are based on or are equivalent to quadratically transforming the data to generate additive sine waves and then applying Fourier analysis in order to detect the resulting *cyclic*

features in the frequency domain. These methods require fine resolution in *cycle frequency* (frequency of a generated sine wave) when long integration time (data record length used in the Fourier analysis) is used [2]. Therefore, in cases of weak-signal detection, where long integration time is needed, and in general search applications, where a search for an unknown signal throughout a wide frequency band is necessary, problems arise in implementation, such as high computational complexity and large amounts of storage and search arise.

This paper introduces two new search-efficient methods of cyclic feature detection, namely the autocorrelated cyclic autocorrelation (ACA) and the autocorrelated cyclic periodogram (ACP). For a given level of detection reliability and computational complexity, implementations of these two methods yield less stringent requirements on resolution in cycle frequency than that of conventional methods of cyclic spectral analysis because the cycle frequency resolution width of these new methods is inherently larger than that of the conventional methods. Therefore, for the detection of weak signals buried in noise within a broad band, the amount of storage and search can be substantially reduced. Once the presence of a cyclic feature is detected and its frequency is estimated using these new methods, a conventional cyclic spectrum analyzer can be used at (and in the vicinity of) this cycle frequency for a finer search and analysis over a much narrower band.

A brief review of cyclic spectral analysis and two conventional methods of cycle detection is given in Section II. The derivation and analysis of the new methods are presented in Section III. A performance comparison of the new and conventional methods is given in Section IV, with computer simulation results being reported in Section V. Finally, concluding remarks are drawn in Section VI.

II. REVIEW OF CYCLIC SPECTRAL ANALYSIS

It has been recognized that many random time series encountered in the field of signal processing are more appropriately modeled as cyclostationary, rather than stationary, due to the underlying periodicities in these signals. An attribute of these cyclostationary time series is that generation of sine waves can be accomplished by subjecting the time series to a stable quadratic time-invariant transformation. The frequencies of these generated sine waves are related to the underlying periodicities and are known as *cycle frequencies* of the signal. Many useful characteristics of cyclostationary signals such as carrier phase, baud timing, information about modulation indices, bandwidth efficiencies, modulation types and, more

Manuscript received June 4, 1994; revised November 6, 1995. This work was supported in part by the National Science Foundation under Grant MIP-91-12800. The associate editor coordinating the review of this work and approving it for publication was Dr. Zhi Ding.

G. K. Yeung is with Mission Research Corporation, Monterey, CA 93940 USA (e-mail: yeung@mrcmry.com).

W. A. Gardner is with the Department of Electrical Engineering, University of California, Davis, CA 95616 USA.

Publisher Item Identifier S 1053-587X(96)03066-8.

generally, degree of spectral redundancy, are reflected in the *cyclic autocorrelation function* and the *spectral correlation function*, which form the basis for cyclic spectral analysis.

The cyclic autocorrelation of a complex-valued time series $x(t)$ is defined by

$$R_x^\alpha(\tau) \triangleq \lim_{T \rightarrow \infty} \frac{1}{T} \int_{-T/2}^{T/2} x(t+\tau/2)x^*(t-\tau/2)e^{-i2\pi\alpha t} dt \quad (1)$$

which can be interpreted as the Fourier coefficient of any additive sine wave component with frequency α that might be contained in the delay product (a quadratic transformation) of $x(t)$.

The spectral correlation function (defined by (5)–(8)), which is also known as the *cyclic spectrum*, can be obtained by Fourier transforming the cyclic autocorrelation

$$S_x^\alpha(f) = \mathcal{F}\{R_x^\alpha(\tau)\} = \int_{-\infty}^{\infty} R_x^\alpha(\tau)e^{-i2\pi f\tau} d\tau. \quad (2)$$

This is the *cyclic Wiener relation* [3]. In the degenerate case of $\alpha = 0$, the left members of (1) and (2) become the conventional autocorrelation function and power spectral density, respectively.

The measurement of the two functions (1) and (2) in signal analysis constitutes what is referred to as *cyclic spectral analysis*. A comprehensive theoretical treatment of this subject is available in Part II of [3], and design and analysis of digital implementations of conventional methods is surveyed in [4]. Here, we review two of the conventional measurement methods, namely the *time-variant finite-average cyclic autocorrelation*, (CA), and the *temporally smoothed cyclic periodogram*, (SCP). The CA and SCP are the conventional counterparts of the new cycle detection methods ACA and ACP, respectively.

The CA of $x(t)$ is defined by

$$R_x^\alpha(t, \tau)_{\Delta t} \triangleq \begin{cases} \frac{1}{\Delta t} \int_{t-\Delta t/2}^{t+\Delta t/2} x(u+\tau/2)x^*(u-\tau/2)e^{-i2\pi\alpha u} du, & |\tau| \leq \Delta t \\ 0, & |\tau| > \Delta t \end{cases} \quad (3)$$

and, for most useful signal and noise models, yields a reliable estimate of the cyclic autocorrelation given in (1) for sufficiently long integration time Δt [3]:

$$\lim_{\Delta t \rightarrow \infty} R_x^\alpha(t, \tau)_{\Delta t} = R_x^\alpha(\tau). \quad (4)$$

As a pointwise limit (in t and τ), (4) is simply definition (1). Reliability means (4) holds also as a limit in temporal (t) mean square [3].

The SCP of $x(t)$ is given by

$$S_{x_{1/\Delta f}}^\alpha(t, f)_{\Delta t} \triangleq \frac{1}{\Delta t} \int_{t-\Delta t/2}^{t+\Delta t/2} S_{x_{1/\Delta f}}^\alpha(u, f) du \quad (5)$$

the integrand of which is the *cyclic periodogram* of $x(t)$ defined by

$$S_{x_T}^\alpha(t, f) \triangleq \frac{1}{T} X_T(t, f + \alpha/2) X_T^*(t, f - \alpha/2) \quad (6)$$

where

$$X_T(t, \nu) \triangleq \int_{t-T/2}^{t+T/2} x(u)e^{-i2\pi\nu u} du \quad (7)$$

is the sliding *finite-time Fourier transform* of $x(t)$. By definition [3]

$$S_x^\alpha(f) \triangleq \lim_{\Delta f \rightarrow 0} \lim_{\Delta t \rightarrow \infty} S_{x_{1/\Delta f}}^\alpha(t, f)_{\Delta t}, \quad (8)$$

and it can be shown [2]–[4] that reliable measurement of the spectral correlation function of $x(t)$, $S_x^\alpha(f)$, using the SCP, can be obtained for $\Delta t \Delta f \gg 1$, where $\Delta f = 1/T$, and that accurate measurement requires small Δf for adequate resolution.

One of the important characteristics of these measurement methods is related to their cycle resolution width, denoted by $\Delta\alpha$. It can be shown [2] that $\Delta\alpha$ of the CA and SCP is on the order of the reciprocal of the total integration time: $\Delta\alpha \cong 1/\Delta t$. That is, cycle frequencies that are closer to each other than $\Delta\alpha = 1/\Delta t$ cannot be resolved. Consequently, for weak-signal detection, where Δt needs to be large, and for general search purposes, where a search over a large range of frequencies is required, the processing of many cycle frequency points is necessary in order not to miss any part of the cyclic spectrum or cyclic autocorrelation. The resulting demand for large search and storage capacities has prompted the need for new methods that would alleviate some of these problems in implementation.

III. DERIVATION AND ANALYSIS

The two new methods of cycle detection presented here are both built, as their names imply, on conventional methods. Specifically, the ACA is obtained by forming the autocorrelation of the time-variant finite-average cyclic autocorrelation and the ACP is obtained by forming the autocorrelation of the time-variant cyclic periodogram. In both methods, the autocorrelation is formed over a total time interval of Δt . However, the finite-average cyclic autocorrelation, and the cyclic periodogram used in these autocorrelations are obtained over a shorter segment of data with length T . The window that selects this segment slides along in time to cover the total time interval of Δt for the autocorrelation operation.

It is shown in [5] and explained in this paper in Section III-A that these new methods have cycle resolution width $\Delta\alpha \cong 1/T$ instead of $\Delta\alpha \cong 1/\Delta t$. Since T can be chosen to be much smaller than Δt for a given level of reliability, $\Delta\alpha$ of the new methods can be much larger than that of the conventional methods. Therefore, the density of cycle frequency samples needed in implementing these new methods is reduced by a factor of $\gamma \triangleq \Delta t/T$, and a reduction by this factor in the amount of storage for the estimates and the amount of search for cyclic features is achieved.

For the derivation and analysis of the ACA and ACP methods, we shall consider the time series model

$$x(t) \triangleq s(t) + n(t) \quad (9)$$

where $s(t)$ is the signal of interest (SOI) that exhibits cyclostationarity and $n(t)$ is purely stationary noise [3]. Since $s(t)$

is assumed to exhibit cyclostationarity, then by definition the lag product

$$y(t) \triangleq x(t + \tau/2)x^*(t - \tau/2) \quad (10)$$

for a continuum of values of lag τ contains finite strength additive sine-wave components and can, therefore, be modeled as

$$y(t) \triangleq \sum_n a_n e^{i2\pi\alpha_n t} + m(t) \quad (11)$$

where the residual is simply the part of $y(t)$ that does not contain sine waves. It follows from definition (10) and model (11) that

$$a_n \equiv R_x^{\alpha_n}(\tau) \equiv R_s^{\alpha_n}(\tau).$$

The problem of detecting the presence of cyclostationarity is therefore the problem of detecting the presence of a family of sine waves indexed by τ in the lag-product waveforms $y(t)$, and the magnitudes and phases of such sine waves are given by $R_x^{\alpha_n}(\tau)$.

It can be shown [1] that this detection is equivalent to the detection of a dc component in the spectral products

$$p(t) = \frac{1}{T} X_T(t, f + \alpha/2) X_T^*(t, f - \alpha/2)$$

for a continuum of values of f and a discrete set of values of α (which is $\{\alpha_n\}$). It follows from definitions (5)–(8) that this dc value is given by

$$\lim_{\Delta t \rightarrow \infty} \frac{1}{\Delta t} \int_{t-\Delta t/2}^{t+\Delta t/2} p(u) du = \lim_{\Delta t \rightarrow \infty} S_{x_T}^{\alpha}(t, f)_{\Delta t}$$

and in the limit, as $T \rightarrow \infty$, this dc value equals $S_x^{\alpha}(f)$. Hence, the problem of detecting cyclostationarity is the problem of detecting the presence of dc components in a family of spectral correlation products indexed by frequency f , for some unknown set of frequency separations α designated by $\{\alpha_n\}$, and the magnitudes and phases of such complex-valued dc components are given by $S_x^{\alpha}(f)$, which is the Fourier transform of $R_x^{\alpha}(\tau)$.

The problem tackled in this paper is that of finding alternatives to the conventional methods for computation of estimates of the families $R_x^{\alpha}(\tau)$ and $S_x^{\alpha}(f)$ of Fourier coefficients and dc values, indexed by (α, τ) and (α, f) , respectively, of quadratic transformations, $y(t)$ and $p(t)$, of the received data $x(t)$. The objective is to find alternatives that are more efficient from a storage and search standpoint, since the size of these families can be extremely large due primarily to the size of the index set for α .

A. The ACA

Using the notation (10) for the delay-product time series, the CA of $x(t)$ for a segment length of T can be expressed as

$$R_x^{\alpha}(t, \tau)_T = \frac{1}{T} \int_{t-T/2}^{t+T/2} y(v) e^{-i2\pi\alpha v} dv, \quad |\tau| \leq T. \quad (12)$$

Forming the correlation of (12) with itself over a total time interval of Δt yields the ACA function

$$R_R(\tau, \alpha; z, U)_{\Delta t} = \frac{1}{\Delta t} \int_{z-\Delta t/2}^{z+\Delta t/2} R_x^{\alpha}(t-U, \tau)_T R_x^{\alpha}(t, \tau)_T^* dt \quad (13)$$

where U is the lag parameter in this autocorrelation and z is the segment index indicating the time location of the segment of data with length $\Delta t + T \cong \Delta t$ (for $\Delta t \gg T$) that is being analyzed.

Without loss of generality, we model $y(t)$ as a sum of sine-wave components plus a residual, as in (11), where the $\{a_n\}$ are the Fourier coefficients of the sine waves generated by the quadratic transformation in (10), the $\{\alpha_n\}$ are the frequencies of the generated sine waves, and $m(t)$ is the residual that does not contain any finite-strength additive sine waves. Using (11) in (12) and substituting (12) into (13), we show in Appendix A that, in the limit as $\Delta t \rightarrow \infty$,

$$\begin{aligned} R_R(\tau, \alpha; U) &\triangleq \lim_{\Delta t \rightarrow \infty} R_R(\tau, \alpha; z, U)_{\Delta t} \\ &= \sum_n |a_n G(\alpha_n - \alpha)|^2 e^{i2\pi(\alpha - \alpha_n)U} \\ &\quad + \frac{1}{T^2} R_M(U) \end{aligned} \quad (14)$$

where

$$G(\beta) = \frac{\sin(\pi\beta T)}{\pi\beta T} \quad (15)$$

$$R_M(U) = \lim_{\Delta t \rightarrow \infty} \frac{1}{\Delta t} \int_{z-\Delta t/2}^{z+\Delta t/2} M_T(t-U, \alpha) M_T^*(t, \alpha) dt \quad (16)$$

and

$$M_T(t, \alpha) = \int_{t-T/2}^{t+T/2} m(v) e^{-i2\pi\alpha v} dv. \quad (17)$$

The sinc window (15) is a result of using a rectangular lag-product tapering window in (12). More generally, $G(\cdot)$ is the Fourier transform of whatever tapering window is used.

Since the cyclic autocorrelation of $x(t)$ can be interpreted as a Fourier coefficient of a sine wave generated by quadratically transforming $x(t)$ according to (10), we have the equivalence $a_n \equiv R_x^{\alpha_n}(\tau)$. Consequently, the limit ACA (with $\Delta t \rightarrow \infty$) can be rewritten as

$$\begin{aligned} R_R(\tau, \alpha; U) &= \sum_n |R_x^{\alpha_n}(\tau) G(\alpha_n - \alpha)|^2 e^{-i2\pi(\alpha_n - \alpha)U} \\ &\quad + \frac{1}{T^2} R_M(U) \end{aligned} \quad (18)$$

where α_n is the n th cycle frequency of the SOI and α is the parameter that is varied in the search.

As a simple example, we assume that the SOI has only one nonzero cycle frequency α_1 and we set the search variable α equal to α_1 . Then, there are only two terms in the sum in (18): $\alpha_n = 0$ and $\alpha_n = \alpha_1$. If the segment length T is chosen to be sufficiently large so that the sinc window $G(\cdot)$, whose width

is on the order of $1/T$, will not pass contributions from the term in the summation with $\alpha_n = 0$, then from (18) we have

$$R_{\bar{R}}(\tau, \alpha_1; U) \cong |R_s^{\alpha_1}(\tau)|^2 + \frac{1}{T^2} R_M(U) \quad (19)$$

since $R_x^{\alpha_1}(\tau) = R_s^{\alpha_1}(\tau)$. If an appropriate value of U is chosen to render the residual term in (19) small compared to the first term, an estimate of the magnitude-squared cyclic autocorrelation of $s(t)$ at α_1 is obtained. Hence, similar to the CA function, the ACA function can also be plotted as a surface over the τ - α plane for the detection of cyclic features for a single value of U .

A slight modification of the ACA that is used throughout the rest of the analysis is introduced here. This modification involves the subtraction of the dc component of $y(t)$ in order to remove the large dc term $R_x^0(\tau)$ in (18). Since all signals, including noise, contribute to $R_x^0(\tau)$, its removal reduces the dynamic range of the ACA surface and eliminates contributions of cycle leakage and noise bias in the ACA measurement [3].

We proceed by defining $\bar{y}(t)$ as the time series obtained by subtracting an estimate of the dc term of $y(t)$ from itself

$$\bar{y}(t) \triangleq y(t) - \frac{1}{T} \int_{t-T/2}^{t+T/2} y(v) dv. \quad (20)$$

As a result, (11) is modified as follows:

$$\bar{y}(t) \triangleq \sum_n \bar{a}_n e^{i2\pi\alpha_n t} + \bar{m}(t) \quad (21)$$

where

$$\begin{aligned} \bar{a}_n &\equiv R_x^{\alpha_n}(\tau) = R_s^{\alpha_n}(\tau), & \alpha_n \neq 0 \\ \bar{a}_n &\equiv 0, & \alpha_n = 0 \end{aligned} \quad (22)$$

and $\bar{m}(t)$ is the resulting residual in $\bar{y}(t)$ that does not contain additive sine waves. The modified ACA becomes

$$\begin{aligned} R_{\bar{R}}(\tau, \alpha; z, U) \Delta t &= \frac{1}{\Delta t} \\ &\times \int_{z-\Delta t/2}^{z+\Delta t/2} \bar{R}_x^\alpha(t-U, \tau)_T \bar{R}_x^\alpha(t, \tau)_T^* dt \end{aligned} \quad (23)$$

where

$$\bar{R}_x^\alpha(t, \tau)_T = \frac{1}{T} \int_{t-T/2}^{t+T/2} \bar{y}(v) e^{-i2\pi\alpha v} dv, \quad |\tau| \leq T. \quad (24)$$

As $\Delta t \rightarrow \infty$, we have

$$\begin{aligned} R_{\bar{R}}(\tau, \alpha; U) &= \sum_{\alpha_n \neq 0} |R_s^{\alpha_n}(\tau) G(\alpha_n - \alpha)|^2 e^{-i2\pi(\alpha_n - \alpha)U} \\ &+ \frac{1}{T^2} R_M(U) \end{aligned} \quad (25)$$

in which $n(t)$ does not make contributions to the first term of (25) because it does not exhibit cyclostationarity $R_x^{\alpha_n}(\tau) = R_s^{\alpha_n}(\tau)$.

It can be shown [5] that the temporal mean, defined for a function $f(t)$ as

$$\lim_{Z \rightarrow \infty} \frac{1}{Z} \int_{-Z/2}^{Z/2} f(s) ds \quad (26)$$

of the ACA function in (23) is given by the right-hand side of (25), the second term of which becomes negligibly small under the weak-signal assumption ($x(t) \cong n(t)$) for $|U| > T + \tau_0$ and $T \gg \tau_0$, where τ_0 is the width of the covariance function for $n(t)$. Therefore, the ACA method can be rendered free of noise bias. Furthermore, the temporal variance, defined for a function $f(t)$ as

$$\lim_{Z \rightarrow \infty} \frac{1}{Z} \int_{-Z/2}^{Z/2} \left[f(s) - \lim_{W \rightarrow \infty} \frac{1}{W} \int_{-W/2}^{W/2} f(u) du \right]^2 ds \quad (27)$$

of the ACA function in (23) under the weak-signal assumption ($x(t) \cong n(t)$) is shown in Appendix B to be

$$\text{var}_{\text{ACA}} \cong \frac{2N_0^4 B^2}{\Delta t T} v_B^2(\alpha) \quad (28)$$

when a complex Gaussian bandlimited white-noise model with bandwidth B ,

$$S_n(f) = \begin{cases} N_0, & |f| \leq B/2 \\ 0, & |f| > B/2 \end{cases} \quad (29)$$

is used and $\Delta t \gg T \gg \tau_0$ is assumed. In (28), $v_B(\alpha)$ is the triangular window

$$v_B(\alpha) \triangleq \begin{cases} 1 - \frac{|\alpha|}{B}, & |\alpha| \leq B \\ 0, & |\alpha| > B. \end{cases} \quad (30)$$

At $\alpha = B$, (28) vanishes because the estimate itself is zero. This is a result of the fact that the quadratic transformation of $n(t)$ does not contain spectral components with frequencies beyond B (cf. (10) and (12)).

It is also shown [5] that the cycle resolution width, $\Delta\alpha$, of the ACA function (given by (13), (18), (23), or (25)) is on the order of $1/T$. An intuitive way of seeing that this is so is to examine (25). Since $R_{\bar{R}}(\alpha, U)$ can be interpreted as a discrete convolution, in α , of $R_s^\alpha(\tau)$ with $G(\alpha)$, the width of $G(\cdot)$, which is on the order of $1/T$, determines the resolution width of $R_{\bar{R}}(\alpha, U)$ in α . Therefore, to obtain the desired feature at α , it is required that there be only one value of α_n for which $|\alpha_n - \alpha| < 1/2T$. In other words, cyclic features that are closer than $1/T$ apart cannot be resolved by the ACA function.

For the case where all the cycle frequencies are farther than $1/T$ apart such that, for each α , there is only one significant term in the summation in the first term of (25), the value of the true cycle frequency α_n can be determined from the phase $2\pi(\alpha_n - \alpha)U$. However, unambiguous recovery of α_n from the phase requires the condition $|\alpha_n - \alpha| < 1/2|U|$. Therefore, with $|\alpha_n - \alpha| < 1/2T$, we have the resulting condition $|U| \leq T$. On the other hand, since the noise bias term in (25) becomes negligible for $|U| > T + \tau_0$ and $T \gg \tau_0$, to determine the value of α_n unambiguously from measurement of the ACA, $U = T$ is used because it comes closest to satisfying $|U| > T + \tau_0$.

Finally, with SNR defined to be the squared magnitude of the mean of the measurement with signal present, normalized by the variance with signal absent, (25) and (28), which are expressions for the mean and variance, respectively, can be used to obtain an expression for the SNR of the ACA method. Specifically, for $\alpha = \alpha_n$, using $U = T$ with $T \gg \tau_0$ and

assuming that only one cyclic feature exists within $\pm 1/2T$ of α and that $n(t)$ is complex stationary bandlimited white Gaussian noise, the SNR of the ACA method is given by

$$\text{SNR}_{\text{ACA}} \cong \frac{\Delta t T |R_s^\alpha(\tau)|^4}{2N_0^4 B^2 v_B^2(\alpha)}, \quad U = T \gg \tau_0, \Delta t \gg T \quad (31)$$

which is used in the performance analysis of the ACA that is presented in Section IV. At $\alpha = B$, the numerator of (31) also vanishes because the signal $s(t)$ does not contain spectral components with frequencies beyond $B/2$, which is a basis for the choice of bandwidth for the bandlimited white-noise $n(t)$.

B. The ACP

The ACP of $x(t)$ is given by

$$R_S(f, \alpha; z, U)_{\Delta t} = \frac{1}{\Delta t} \int_{z-\Delta t/2}^{z+\Delta t/2} S_{x_T}^\alpha(t, f) S_{x_T}^\alpha(t-U, f)^* dt \quad (32)$$

where $S_{x_T}^\alpha(t, f)$ is the cyclic periodogram given by (6).

Without loss of generality, $p(t) \triangleq S_{x_T}^\alpha(t, f)$ can be modeled as follows:

$$p(t) \triangleq \sum_n b_n e^{i2\pi\beta_n t} + q(t) \quad (33)$$

where the $\{b_n\}$ are the Fourier coefficients of the additive sine waves contained in $p(t)$, the $\{\beta_n\}$ are the frequencies of these sine waves, and $q(t)$ is the residual that does not contain any finite-strength additive sine waves. It is shown [5] that the coefficients b_n are given by

$$b_n = S_x^{\alpha+\beta_n}(f) \otimes H_{\beta_n}(f) \quad (34)$$

where

$$H_\beta(f) = \frac{1}{T} A_{1/T} \left(f + \frac{\beta}{2} \right) A_{1/T}^* \left(f - \frac{\beta}{2} \right) \quad (35)$$

and $A_{1/T}(f)$ is the Fourier transform of the data tapering window $a_T(t)$ (which is just a rectangular window in the simplest case illustrated by (7)). We see from (34) that $\alpha + \beta_n = \alpha_n$ is the n th cycle frequency of $x(t)$.

In the limit as $\Delta t \rightarrow \infty$, we have

$$\begin{aligned} R_S(f, \alpha; U) &\triangleq \lim_{\Delta t \rightarrow \infty} R_S(f, \alpha; z, U)_{\Delta t} \\ &= \sum_n |S_x^{\alpha_n}(f) \otimes H_{\alpha_n-\alpha}(f)|^2 e^{i2\pi(\alpha_n-\alpha)U} \\ &\quad + R_q(U). \end{aligned} \quad (36)$$

As a result, similar to the SCP, the ACP function can be plotted as a surface over the f - α plane (for a single value of U) for the detection of cyclic features.

To remove the large dc term $S_x^0(f)$, the sine-wave component with frequency $\beta_n = -\alpha$ in $p(t)$ is subtracted. Therefore, we define

$$\bar{p}(t) \triangleq p(t) - \frac{1}{T} \int_{t-T/2}^{t+T/2} p(v) e^{i2\pi\alpha v} dv \quad (37)$$

such that the resulting ACP

$$R_{\bar{S}}(f, \alpha; z, U)_{\Delta t} = \frac{1}{\Delta t} \int_{z-\Delta t/2}^{z+\Delta t/2} \bar{p}(t) \bar{p}^*(t-U) dt \quad (38)$$

approaches, in the limit as $\Delta t \rightarrow \infty$,

$$\begin{aligned} R_{\bar{S}}(f, \alpha; U) &= \sum_{\alpha_n \neq 0} |S_s^{\alpha_n}(f) \otimes H_{\alpha_n-\alpha}(f)|^2 e^{i2\pi(\alpha_n-\alpha)U} \\ &\quad + R_{\bar{q}}(U) \end{aligned} \quad (39)$$

where $n(t)$ does not have contributions to the first term of (39) because $S_x^{\alpha_n}(f) = S_s^{\alpha_n}(f)$.

It is shown in [5] that the temporal mean of the ACP function in (38) is given by the right-hand side of (39), the second term of which becomes negligibly small for $|U| > T$ and $n(t)$ consisting of stationary complex Gaussian noise, thereby rendering the ACP method free of noise bias. Furthermore, the temporal variance of the ACP method under the weak-signal assumption ($x(t) \cong n(t)$) is shown, in a fashion similar that used to obtain (28), to be

$$\text{var}_{\text{ACP}} \cong \frac{2N_0^4 T}{5\Delta t} \quad (40)$$

for $\Delta t \gg T \gg \tau_0$ and $n(t)$ consisting of stationary complex Gaussian noise. Finally, similar to the ACA method, the cycle resolution width of the ACP method is shown in [5] to be $1/T$. Consequently, choosing $U = T$ for both minimal noise bias and unambiguous recovery of α_n from the phase, setting $\alpha = \alpha_n$, and assuming that $n(t)$ is stationary complex Gaussian noise and that only one cyclic feature exists within $\pm 1/2T$ of α , (39) and (40) can be used to obtain the following SNR expression for the ACP method:

$$\text{SNR}_{\text{ACP}} \cong \frac{5\Delta t}{2N_0^4 T} |S_s^\alpha(f) \otimes z_{1/T}(f)|^4, \quad \Delta t \gg T \gg \tau_0 \quad (41)$$

where

$$z_{1/T}(f) = \frac{1}{T} \left| \frac{\sin(\pi f T)}{\pi f} \right|^2 \quad (42)$$

is a result of using a rectangular data-tapering aperture in (7). More general expressions for (42) are obtained using (35) with $\beta = 0$.

IV. PERFORMANCE COMPARISON

Computational counts, search savings, and output SNR expressions are used in this section to compare performances of the ACA, CA, ACP, and SCP methods. Without constraining the total amount of data processed by each method to be the same, (31) and (41) together with results from [6] yield, for $\alpha = \alpha_n$ and $n(t)$ stationary complex Gaussian,

$$\text{SNR}_{\text{ACA}} \cong \frac{\Delta t_{\text{ACA}} T B^2 \rho_A^4}{2(1-|\alpha|/B)^2}, \quad \Delta t \gg T \gg \tau_0 \quad (43)$$

$$\text{SNR}_{\text{CA}} \cong \frac{\Delta t_{\text{CA}} B \rho_A^2}{K_A(1-|\alpha|/B)}, \quad \Delta t \gg \tau_0 \quad (44)$$

$$\text{SNR}_{\text{ACP}} \cong \frac{5\Delta t_{\text{ACP}} \rho_P^4}{2T}, \quad \Delta t \gg T \gg \tau_0 \quad (45)$$

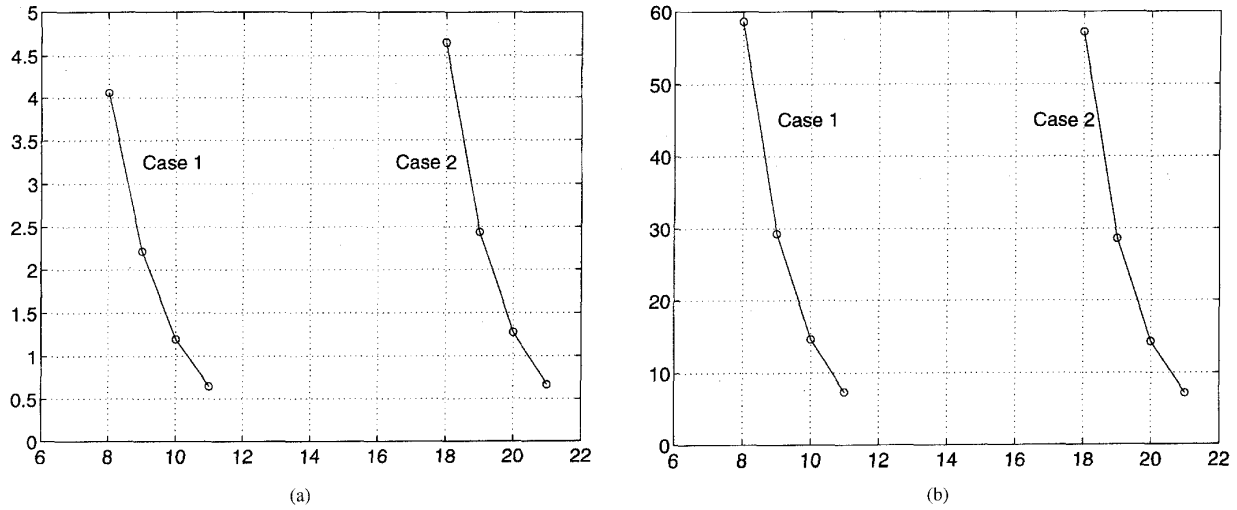


Fig. 1. Equal-output-SNR performance comparison of the ACA and CA methods for $\text{SNR}_{\text{OUT}} = 10$ dB and $\rho_A = -15$ dB (Case 1), $\rho_A = -30$ dB (Case 2). (a) η_A versus $\log_2(Tf_s)$. (b) γ_A versus $\log_2(Tf_s)$.

and

$$\text{SNR}_{\text{SCP}} \cong \frac{\Delta t_{\text{SCP}} \rho_P^2}{K_P T}, \quad \Delta t \gg T \quad (46)$$

where

$$\rho_A \triangleq \frac{|R_s^\alpha(\tau)|}{BN_0}, \quad (47)$$

$$\rho_P \triangleq \frac{|S_s^\alpha(f) \otimes z_{1/T}(f)|}{N_0}, \quad (48)$$

$$K_A = \begin{cases} 2, & |\tau| \ll (B - |\alpha|)^{-1}, \alpha \neq 0 \\ 1, & \text{otherwise} \end{cases} \quad (49)$$

and

$$K_P = \begin{cases} 2, & |f| \ll 1/T \\ 1, & \text{otherwise.} \end{cases} \quad (50)$$

Both the ACA and ACP methods yield output SNR's that are proportional to their corresponding input SNR (ρ) raised to the fourth power, whereas those of the CA and SCP methods are proportional to only the square of the input SNR. This illustrates the fact that, for very low input SNR ($\rho < 1$), output SNR degrades as the order of nonlinear transformation of the data increases. Despite this fact, the ACA method is shown, both theoretically and experimentally, to be more promising than the ACP method and to have performance that is comparable to that of the CA and SCP methods. Recall that methods for measuring the CA yield processing gain proportional to the integration time, whereas those for measuring the cyclic periodogram do not [3]; hence, the ACA has a processing gain of $\Delta t TB^2$, whereas the ACP has a processing gain of only $\Delta t/T$ (cf. (43)–(46)). As a result, the ACA method yields an extra processing gain factor of TB compared to the CA method and an extra processing gain factor of $(TB)^2$ compared to the ACP and SCP methods. For narrowband signals, this extra processing gain compensates for the smaller values of ρ_A compared with ρ_P (cf. (47) and (48)) as a result of the fact that $S_s^\alpha(f)$ for narrowband signals has relatively higher peaks than does $R_s^\alpha(\tau)$.

The two measures of performance comparison used here are based on the constraints of equal-output-SNR and equal-search requirements. For equal output SNR, performance comparison of the ACA and CA methods in terms of computational cost ratio (η_A) and search savings factor (γ_A) can be obtained by equating (43) and (44) to obtain a relationship between Δt_{ACA} and Δt_{CA} (the amounts of data processed by the ACA and CA methods) and substituting this relationship into the formulas

$$\eta_A = \frac{2\Delta t_{\text{ACA}}[\log_2(Tf_s) + 3]}{\Delta t_{\text{CA}}[\log_2(\Delta t_{\text{CA}} f_s) + 2]} \quad (51)$$

and

$$\gamma_A = \frac{\Delta t_{\text{CA}}}{T} \quad (52)$$

where η_A is defined to be the ratio of the number of real multiplications used to obtain the ACA to that used to obtain the CA, search savings factor γ_A is defined to be the ratio of the cycle resolution widths of the ACA and CA methods, and f_s is the sampling frequency used in the digital system [5]. Fig. 1 shows η_A and γ_A versus Tf_s for an equal-output-SNR of 10 dB, $\alpha = 0.25f_s$, $\tau = 0$, and $B = f_s$ for the two cases: $\rho_A = -15$ dB and $\rho_A = -30$ dB. Although search savings is gained at the expense of computational efficiency, by choosing an appropriate value of T , search savings can still be obtained without an increase in computation compared to the conventional method in these cases of very low input SNR.

Similarly, equating (45) and (46) for equal-output-SNR and substituting the resultant relationship between Δt_{ACP} and Δt_{SCP} into the formulas

$$\eta_P = \frac{\Delta t_{\text{ACP}}[\log_2(Tf_s) + 4]}{\Delta t_{\text{SCP}}[\log_2(Tf_s) + 2]} \quad (53)$$

and

$$\gamma_P = \frac{\Delta t_{\text{SCP}}}{T} \quad (54)$$

where η_P is defined to be the ratio of the number of real multiplications used to obtain the ACP to that used to obtain

the SCP, and γ_P is the search savings factor for the ACP over the SCP, we observe that for a given input SNR and desired output SNR, γ_P is constant, whereas η_P varies with T . For example, for an equal-output-SNR of 10 dB with $f = 0$, $B = f_s$, and $Tf_s = 2^{13}$, $\gamma_P \cong 80$ and $\eta_P \cong 0.9$ for $\rho_P = -3$ dB, and $\gamma_P = 2000$ and $\eta_P \cong 23$ for $\rho_P = -10$ dB. Search savings increases with decreasing input SNR due to the fact that a larger $\Delta t/T$ ratio is required to obtain a certain level of output SNR when input SNR is decreased. On the other hand, as the input SNR decreases, computational cost η_P increases for the ACP to achieve the same SNR performance as the conventional method.

The second measure of performance considered is based on the constraint of equal search-performance. If the search size for cyclic features in both the new and conventional methods is constrained to be the same by averaging measurements over $\gamma = \Delta t/T$ adjacent cycle frequency samples in the conventional method, then the output SNR of the conventional method is reduced by a factor of γ . Therefore, the resulting SNR is given by

$$\text{SNR}' \triangleq \frac{\text{SNR}}{\gamma}. \quad (55)$$

Defining G_A to be the gain in output SNR due to using the ACA method, we have

$$G_A \triangleq \frac{\text{SNR}_{ACA}}{\text{SNR}'_{CA}} = \frac{K_A^2 \Delta t_{ACA}}{2T} \text{SNR}'_{CA} \quad (56)$$

where G_A is guaranteed to be greater than one for SNR'_{CA} larger than two. Therefore, the ACA method provides a better solution for reduction of search by yielding a higher output SNR than the method of averaging adjacent measurements.

Similarly, for the ACP method, we have

$$G_P \triangleq \frac{\text{SNR}_{ACP}}{\text{SNR}'_{SCP}} = \frac{5\Delta t_{ACP}\rho_P^2 K_P}{2T} \quad (57)$$

which increases with $\Delta t_{ACP}/T$ for a given input SNR. Hence, G_P can be made greater than one by choosing $\Delta t_{ACP}/T$ large.

V. COMPUTER SIMULATIONS

For the computer simulations presented in this section, the SOI is a random binary pulse-amplitude-modulated (PAM) time series with 100% excess-bandwidth Nyquist-shaped pulses and $n(t)$ is a complex random time series with Gaussian probability distributions. A baud-rate of $f_b = 0.25f_s$ is used in the illustration of surfaces and $f_b = f_s/3$ is used in obtaining the receiver operating characteristics. A sampling frequency of $f_s = 1$ is used in all simulations.

Magnitude surfaces of the ACA and the CA of $x(t)$ with $\text{SNR}_{IN} = 0$ dB (SNR_{IN} = ratio of signal power to noise power), $\Delta t f_s = 8192$, and $T f_s = 256$ (for the ACA) are shown in Figs. 2 and 3, respectively. Baud-rate features at $\alpha = \pm 0.25$ can be easily identified in both plots. Magnitude surfaces of the ACP and the SCP of $x(t)$ with $\text{SNR}_{IN} = 0$ dB, $\Delta t f_s = 65536$, and $T f_s = 64$ are shown in Figs. 4 and 5, respectively. The phenomenon of cycle leakage is especially evident in the case of the ACP surface. This can be explained

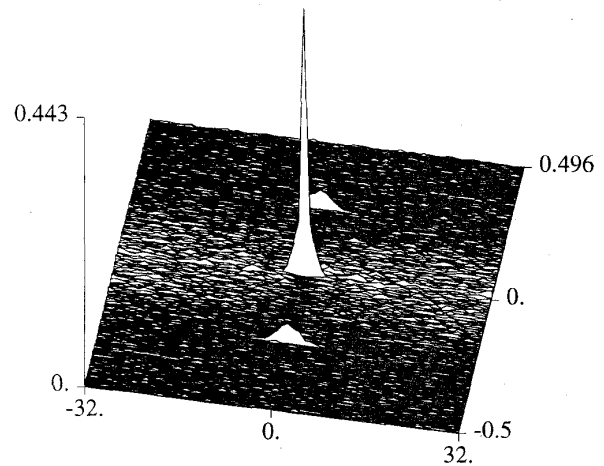


Fig. 2. Magnitude of the ACA for $\text{SNR}_{IN} = 0$ dB, $\Delta t f_s = 8192$, $T f_s = 256$, $f_b = 0.25 f_s$, and $f_s = 1$.

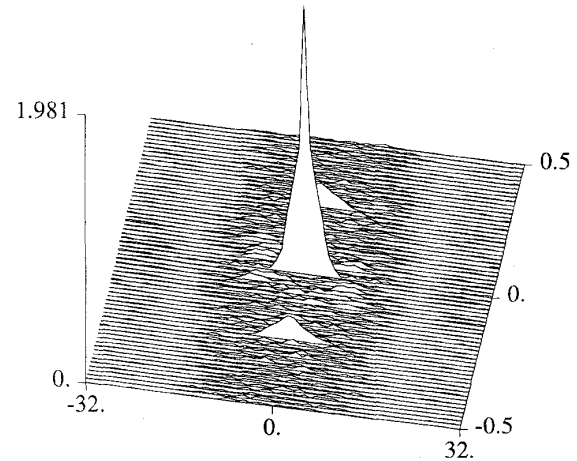


Fig. 3. Magnitude of the CA for $\text{SNR}_{IN} = 0$ dB, $\Delta t f_s = 8192$, $f_b = 0.25 f_s$, and $f_s = 1$.

by examining (18) and (36), in which the rates of decay in β of the window functions (15) and (35) determine the amount of cycle leakage in the corresponding methods. Since the rate of decay in β of (35) for a rectangular data-tapering window is smaller than that of (15), the contribution of cycle leakage is larger for the ACP method. In addition, for the parameters (f_b, B, T) used in this simulation, a longer data collect time, compared to that used in the ACA and CA methods, is needed for both the ACP and SCP methods to yield surfaces of the quality shown. This agrees with the results in [6] of comparing f -based and τ -based cyclic spectral analysis methods. In general, the relative superiority of τ -based methods and f -based methods depends on the parameters f_b , B , and T , as can be seen in (43)–(48). (In some instances, the collect time needed for the CA can be longer than that needed for the SCP.)

Detection performance of the ACA method is compared to that of the CA and SCP methods by means of the receiver operating characteristic (ROC), which is a graph of probability of detection versus probability of false alarm. Detection

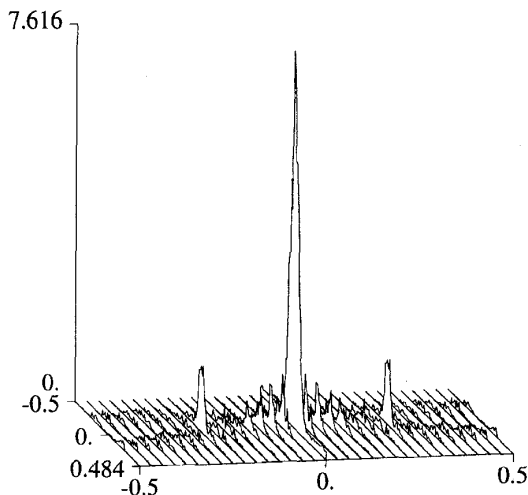


Fig. 4. Magnitude of the ACP for $\text{SNR}_{\text{IN}} = 0$ dB, $\Delta t f_s = 65\,536$, $T f_s = 64$, $f_b = 0.25 f_s$, and $f_s = 1$.

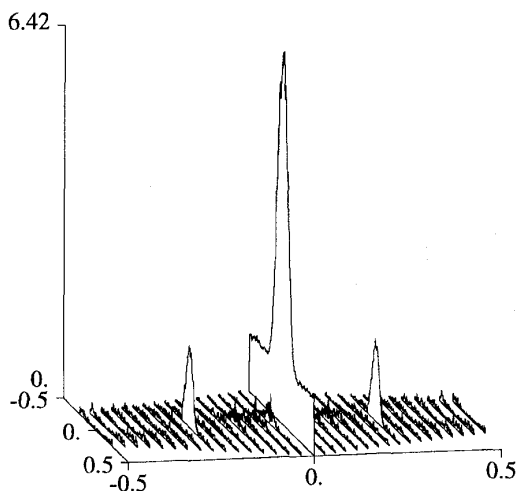


Fig. 5. Magnitude of the SCP for $\text{SNR}_{\text{IN}} = 0$ dB, $\Delta t f_s = 65\,536$, $T f_s = 64$, $f_b = 0.25 f_s$, and $f_s = 1$.

performance of the ACP method is not evaluated due to its inferiority relative to the ACA method. For the PAM signal considered in these simulations, it is known that the baud-rate features peak at $\tau = 0$ for the ACA and CA, and at $f = 0$ for the ACP and SCP. Therefore, the detection procedure used here involves searches over cycle frequency α at only $\tau = 0$ for the ACA and CA, and only $f = 0$ for the SCP. The detection statistic is the magnitude of the corresponding surface. Note that $\alpha = k/T$, where k is an integer, is used in the new methods and $\alpha = m/\Delta t$, where m is an integer, is used in the conventional methods. Therefore, for $f_b = f_s/3$, none of the cycle frequency samples used in obtaining the ROC's fall exactly on $\alpha_n = f_b$. On the other hand, $\alpha = \alpha_n$ is used in the expressions for output SNR in Section IV. Hence, the ROC performance presented here is not meant to be compared directly with the SNR expressions. Fig. 6 shows ROC's of the ACA and CA methods for $\text{SNR}_{\text{IN}} = -13$

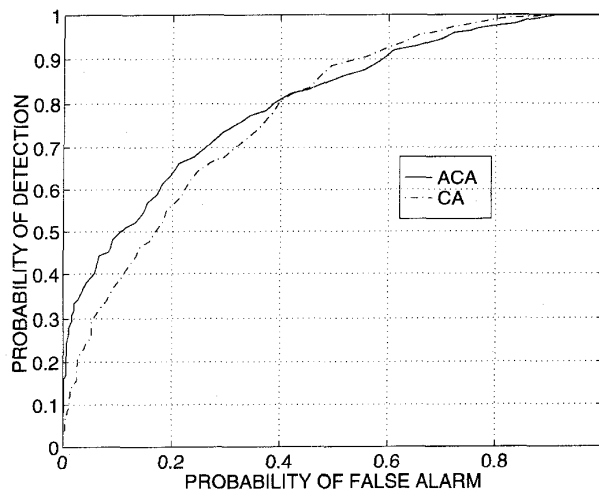


Fig. 6. ROC's for $\text{SNR}_{\text{IN}} = -13$ dB, $\Delta t f_s = 131\,072$, $T f_s = 16\,384$, and $f_b = f_s/3$.

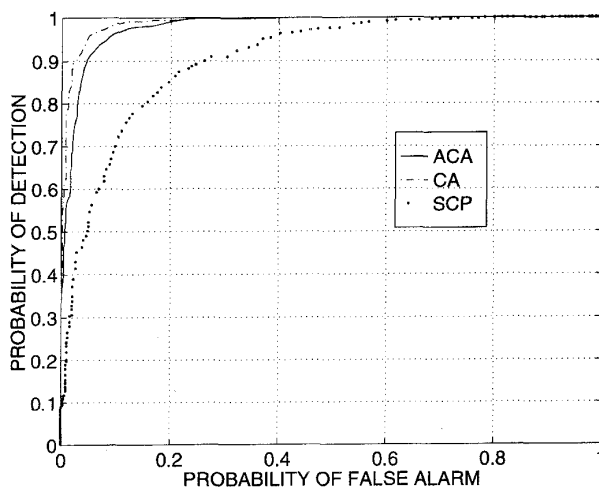


Fig. 7. ROC's for $\text{SNR}_{\text{IN}} = -5$ dB, $\Delta t f_s = 4\,096$, $T f_s = 256$, and $f_b = f_s/3$.

dB, $\Delta t f_s = 131\,072$, and $T f_s = 16\,384$ (for the ACA). Detection performance of both methods are comparable in this weak-signal environment, while search/storage requirements for the ACA are reduced by a factor of eight relative to the requirements for the CA. For $\text{SNR}_{\text{IN}} = -5$ dB, $\Delta t f_s = 4\,096$, and $T f_s = 256$, both the ACA and CA methods are superior to the SCP as shown in Fig. 7. For $\text{SNR}_{\text{IN}} = 0$ dB, all three methods perform very well with $\Delta t f_s = 4\,096$ and $T f_s = 256$ as shown in Fig. 8.

VI. CONCLUSION

The analyses and simulations of the ACA and ACP methods show that their SNR performance can be comparable to that of their conventional counterparts while a considerable amount of search and storage savings is achieved, or, for equal search/storage performance, considerable gains in output SNR can be achieved. Moreover, the ACA method performs

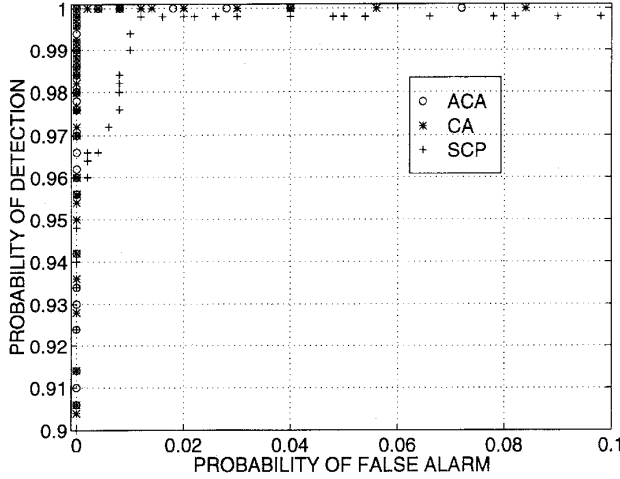


Fig. 8. ROC's for $\text{SNR}_{\text{IN}} = 0$ dB, $\Delta t f_s = 4096$, $T f_s = 256$, and $f_b = f_s/3$.

better than the ACP method in weak-signal environments due to the extra processing gain provided by the ACA and the smaller amount of cycle leakage exhibited. Therefore, the ACA method proves to be superior to the ACP method in weak-signal detection even though for general search applications, where a search throughout a large range of cycle frequencies is required, the ACP is still a better solution than the conventional methods with regard to search savings.

Besides attaining the goal of reduction in search for a given level of performance reliability, the new methods also provide information on the true cycle frequency. Frequency location and phase of the detected feature can be used to obtain an estimate of α_n . To balance the various advantages, there are two limitations associated with the new methods. First, multiple sine waves that are less than $1/T$ apart cannot be resolved without using a conventional method for finer local resolution after detection has been accomplished with one of the new methods. Second, for a given amount of data and very low input SNR, measurements obtained from higher order nonlinear transformation degrade compared to measurements of equivalent lower order transformation. For the ACP method, longer integration time is required to maintain the same level of performance reliability as input SNR decreases, thereby increasing computational cost. For the ACA method, due to the extra processing gain, search savings can still be obtained without an increase in computational cost compared to the conventional method even in the case of $\rho_A = -30$ dB. Therefore, the ACA method proves to be promising in search-efficient detection of weak cyclostationary signals.

APPENDIX A

DERIVATION OF THE LIMIT ACA FUNCTION IN (14)

Using (11) in (12), we arrive at

$$R_x^\alpha(t, \tau)_T = \sum_n a_n G(\alpha_n - \alpha) e^{i2\pi(\alpha_n - \alpha)t} + M_T(t, \alpha) \quad (58)$$

where $G(\beta)$ and $M_T(t, \alpha)$ are given by (15) and (17), respectively. Substituting (58) into (13) and interchanging summations and integrations together with some change of variables, we obtain the following expression for the ACA:

$$R_R(\tau, \alpha; z, U)_{\Delta t} = \text{Term1} + \text{Term2} + \text{Term3} + \text{Term4} \quad (59)$$

where

$$\begin{aligned} \text{Term1} &= \sum_n \sum_m a_n a_m^* G(\alpha_n - \alpha) G(\alpha_m - \alpha) \\ &\quad \times w_{1/\Delta t}(\alpha_n - \alpha_m) e^{i2\pi(\alpha - \alpha_n)U} e^{i2\pi(\alpha_n - \alpha_m)z} \end{aligned} \quad (60)$$

$$\begin{aligned} \text{Term2} &= \frac{1}{\Delta t T} \sum_n a_n G(\alpha_n - \alpha) \\ &\quad \times \int_{-T/2}^{T/2} M_{\Delta t}^*(z + v, \alpha_n) e^{i2\pi(\alpha - \alpha_n)(U+v)} dv \end{aligned} \quad (61)$$

$$\begin{aligned} \text{Term3} &= \frac{1}{\Delta t T} \sum_m a_m^* G(\alpha_m - \alpha) \\ &\quad \times \int_{-T/2}^{T/2} M_{\Delta t}(z + v - U, \alpha_m) e^{i2\pi(\alpha - \alpha_m)(U-v)} dv \end{aligned} \quad (62)$$

$$\text{Term4} = \frac{1}{\Delta t T^2} \int_{z-\Delta t/2}^{z+\Delta t/2} M_T(t - U, \alpha) M_T^*(t, \alpha) dt \quad (63)$$

and

$$w_{1/\Delta t}(\beta) = \frac{\sin(\pi\beta\Delta t)}{\pi\beta\Delta t}. \quad (64)$$

In the limit as $\Delta t \rightarrow \infty$, the second and third terms go to zero because the residual $m(t)$ in $M_{\Delta t}(t, \alpha)$ is uncorrelated with all sine waves. Hence, we arrive at the limit ACA function given by (14).

APPENDIX B

DERIVATION OF THE VARIANCE OF THE ACA FUNCTION IN (23) FOR THE WEAK-SIGNAL MODEL: $x(t) = n(t)$

It can be shown that for the weak-signal model, $\bar{y}(t)$ (given by (20) and (21)) equals $\bar{m}(t)$. Therefore, using (17) and (24) in (23), the ACA in (23) becomes

$$\begin{aligned} R_{\bar{R}}(\tau, \alpha; z, U)_{\Delta t} &= \frac{1}{\Delta t T^2} \int_{z-\Delta t/2}^{z+\Delta t/2} \bar{M}_T(t - U, \alpha) \bar{M}_T^*(t, \alpha) dt. \end{aligned} \quad (65)$$

Replacing $f(s)$ in (27), the definition for the variance of $f(s)$, with (65), assuming that $n(t)$ is purely stationary of all orders such that the residual $\bar{m}(t)$ does not contain any second order periodicity, and using a Gaussian approximation to the time series $\bar{M}_T(t, \alpha)$ (which is a good approximation under the condition that $T \gg \tau_0$), we arrive at the expression for the variance of the ACA [5] as follows:

$$\text{var}_{\text{ACA}} \cong \frac{1}{\Delta t T^4} \int_{-\infty}^{\infty} v_{\Delta t}(s) |R_{\bar{M}}(s)|^2 ds, \quad T \gg \tau_0 \quad (66)$$

where $v_{\Delta t}(\cdot)$ is the triangular window given by (30), with B replaced by Δt , and $R_{\bar{M}}(s)$ can be expressed as

$$R_{\bar{M}}(s) = T \int_{-\infty}^{\infty} v_T(u+s) R_{\bar{m}}(u) e^{-i2\pi\alpha u} du \quad (67)$$

using definitions (16) and (17).

By using Isserlis' formula for the fourth-order joint moment of a Gaussian time series, the autocorrelation function of the residual $\bar{m}(t)$ can be expressed in terms of the autocorrelation of the noise $n(t)$ as follows:

$$R_{\bar{m}}(u) \cong |R_n(u)|^2 + R_{nn^*}(u+\tau) R_{nn^*}^*(u-\tau), \quad (68)$$

for $T \gg \tau_0$. Substituting (68) into (67) and the result into (66) using Fourier transform relations, and evaluating the integral assuming $\Delta t \gg T \gg \tau_0$, we obtain

$$\text{var}_{\text{ACA}} \cong \frac{2}{\Delta t T} |S_{\bar{m}}(\alpha)|^2. \quad (69)$$

Since $R_{nn^*}(u) \equiv 0$ for complex Gaussian noise, the second term of (68) vanishes and the final expression of the variance of the ACA becomes, using (68) in (69), the following:

$$\text{var}_{\text{ACA}} \cong \frac{2N_0^4 B^2}{\Delta t T} v_B^2(\alpha) \quad (70)$$

for $\Delta t \gg T \gg \tau_0$ and complex Gaussian bandlimited white-noise with bandwidth B and power spectral density N_0 .

REFERENCES

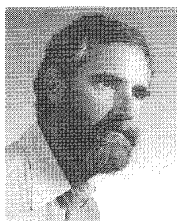
- [1] W. A. Gardner, "Signal interception: A unifying theoretical framework for feature detection," *IEEE Trans. Commun.*, vol. 36, pp. 897-906, Aug. 1988.
- [2] ———, "Measurement of spectral correlation," *IEEE Trans. Acoust., Speech, Signal Processing*, vol. ASSP-34, pp. 1111-1123, Oct. 1986.
- [3] ———, *Statistical Spectral Analysis: A Nonprobabilistic Theory*. Englewood Cliffs, NJ: Prentice-Hall, 1987.
- [4] R. S. Roberts, W. A. Brown, and H. H. Loomis, Jr., "A review of digital spectral correlation analysis: Theory and implementation," in *Cyclostationarity in Communications and Signal Processing*, W. A. Gardner, Ed. Piscataway, NJ: IEEE, 1994.
- [5] G. K. Yeung, "New methods of cycle detection," Master's thesis, Dep. Elect. Comput. Eng., Univ. California, Davis, June 1991.
- [6] C. M. Spooner and W. A. Gardner, "A performance comparison of two signal analysis surfaces: ambiguity and spectral correlation," tech. rep. 92-1, Dep. Elect. Comput. Eng., Univ. of Calif., Davis, 1992.



Grace K. Yeung was born in Hong Kong in 1968. She received the B.S. and M.S. degrees in electrical engineering from the University of California, Davis, in 1990 and 1993, respectively.

She was a teaching assistant in the Department of Electrical and Computer Engineering at U. C. Davis from 1991 to 1992. From 1992 to 1993, she was a research assistant at U. C. Davis and a consultant to Statistical Signal Processing, Inc., Yountville, CA. Since August 1993, she has been a member of the technical staff at Mission Research Corporation, Monterey, CA, engaged in work on blind-adaptive frequency-shift filtering as well as detection, classification, and separation of cyclostationary signals. Her research interests include statistical signal processing, modulation classification, new methods of cyclostationary-signal detection for efficient storage and search, and cubic frequency-shift filtering for bandwidth-efficient signals.

Ms. Yeung received the Departmental Citation Award from the Department of Electrical and Computer Engineering at U. C. Davis in 1990, and is a member of Tau Beta Pi Engineering, Pi Mu Epsilon Mathematics, and Golden Key National Honor Societies.



William A. Gardner (S'64-M'67-SM'84-F'91) was born in Palo Alto, CA, in 1942. He received the M.S. degree from Stanford University, Stanford, CA, in 1967, and the Ph.D. degree from the University of Massachusetts, Amherst, in 1972, both in electrical engineering.

He was a Member of the Technical Staff at Bell Laboratories in Massachusetts from 1967 to 1969. He has been a faculty member at the University of California, Davis, since 1972, where he is professor of electrical and computer engineering. Since 1982, he has also been president of the engineering consulting firm Statistical Signal Processing, Inc., Yountville, CA. His research interests are in the general area of statistical signal processing, with primary emphasis on the theories of time-series analysis, stochastic processes, and signal detection and estimation, and applications to communications and signals intelligence. He is the author of *Introduction to Random Processes with Applications to Signals and Systems*, (New York, Macmillan, 1985; 2nd ed., New York: McGraw-Hill, 1990), *The Random Processes Tutor: A Comprehensive Solutions Manual for Independent Study*, (New York, McGraw-Hill, 1990), and *Statistical Spectral Analysis: A Nonprobabilistic Theory*, (Englewood Cliffs, NJ: Prentice-Hall, 1987). He is also editor of *Cyclostationarity in Communications and Signal Processing*, (New York, IEEE Press, 1994). He holds several patents and is the author of numerous research journal papers.

Dr. Gardner received the Best Paper of the Year Award from the European Association for Signal Processing in 1986, the 1987 Distinguished Engineering Alumnus Award from the University of Massachusetts, and the Stephen O. Rice Prize Paper Award in the Field of Communication Theory from the IEEE Communications Society, 1988. He organized and chaired the NSF/ONR/ARO/AFOSR-sponsored Workshop on Cyclostationary Signals in 1992. He is a member of the American Association for the Advancement of Science as well as the European Association for Signal Processing, and is a member of the honor societies Sigma Xi, Tau Beta Pi, Eta Kappa Nu, and Alpha Gamma Sigma. He was elected Fellow of the IEEE in 1991 "for contributions to the development of time-series analysis and stochastic processes with applications to statistical signal processing and communication, and for contributions to engineering education."